Digalloyl Glycoside: A Potential Inhibitor of Trypanosomal PFK

Subjects: Pharmacology & Pharmacy

Contributor: Elham Amin

Human African trypanosomiasis is an endemic infectious disease caused by *Trypanosoma brucei* via the bite of tsetse-fly. Most of the drugs used for the treatment, e.g., Suramin, have shown several problems, including the high level of toxicity. A phytochemical investigation of the methanolic extract of *E. abyssinica* was carried out. Twelve compounds, including two triterpenes (1, 2); one sterol-glucoside (4); three ellagic acid derivatives (3, 9, 11); three gallic acid derivatives (5, 6, 10); and three flavonoids (7, 8, 12), were isolated. Compound (10) was obtained for the first time from genus *Euphorbia* while all other compounds except compound (4), were firstly reported in *E. abyssinica*. Consequently, an *in silico* study was used to estimate the anti-trypanosomal activity of the isolated compounds. Several compounds displayed interesting activity where 1,6-di-*O*-galloyl-d-glucose (10) appeared as the most potent inhibitor of trypanosomal phosphofructokinase (PFK). Moreover, molecular dynamics (MD) simulations and ADMET calculations were performed for 1,6-di-*O*-galloyl-d-glucose. In conclusion, 1,6-di-*O*-galloyl-d-glucose revealed high binding free energy, desirable molecular dynamics, and pharmacokinetic properties; therefore, it could be suggested for further *in vitro* and *in vivo* studies for trypanosomiasis.

Trypanosoma brucei | Euphorbia abyssinica | in silico | 6-di-O-galloyl-d-glucose | molecular dynamics | ADMET

1. Introduction

Trypanosoma brucei is the causative agent of human African trypanosomiasis (HAT), sleeping sickness, via the bite of the tsetse fly. One of the most druggable target enzymes for the treatment of HAT is the trypanosomal phosphofructokinase (PFK) enzyme [1]. Suramin, a classic PFK inhibitor, is known to exhibit significant side effects such as hypersensitivity, agranulocytosis, and nephrotoxicity [2].

E. abyssinica J.F. Gmel latex was reported to yield ingenol esters and lathyrane derivatives as minor components besides euphol, euphorbol, lupeol, oleanolic acid, β-sitosterol, and β-sitosterol-3-*O*-glucoside. Also, it has shown significant antifungal activity against *Aspergillus flavus, Aspergillus niger,* and *Candida albicans* [3]. Furthermore, *E. abyssinica* has exhibited cytotoxic activity against Caco2 (IC_{50} 11.3 µg/mL) [4]. Moreover, the root of *E. abyssinica* has shown potent chemosuppressive antimalarial activity against *Plasmodium berghei* infection in mice [5].

Recently, molecular docking is important in the estimation of the bioactivity of chemical compounds against a target and has shown great progress [6]. The evaluation of drug design depends on the identification and characterization of small-molecule binding sites on the target proteins [7].

In our previous research, the anti-trypanosomal activity of the methanolic extract of *E. abyssinica* against *T. brucei brucei* strain TC221 was investigated, and IC_{50} values were determined as 17.3 and 19.4 µg/mL after 48 and 72 h incubation, respectively [8]. Consequently, the current study discusses the molecular modeling study of the compounds isolated from *E. abyssinica* J.F. Gmel. against the target proteins (PFK) of *T. brucei.* Furthermore, the molecular dynamics and pharmacokinetic properties of the most active compound are also presented in order to conclude the compound activity.

2. Investigation of Methylene Chloride Fraction of *E. abyssinica* J.F. Gmel

Chromatographic investigation of methylene chloride fraction led to isolation of four compounds. The structure of the isolated compounds was elucidated using 1D NMR and LC-HRMS. Compound (**1**): White needle powder (15 mg), m.p. 208–212 °C, gave a positive Libermann–Burchard's test indicating its steroidal or triterpenoidal nature. LC-HRMS $[M + H]^+$ *m/z*: 427.3931, R_t: 26.12 calculated for $C_{30}H_{50}O$. ^{1}H-NMR (400 MHz) and DEPT-Q NMR (100 MHz) in CD_3OD.

Compound (**2**): White crystal powder (25 mg), m.p. 282–285 °C, gave a positive Libermann–Burchard's test indicating its steroidal or triterpenoidal nature. LC-HRMS $[M + H]^-$ *m/z*: 425.3859, R_t: 28.97 calculated for $C_{30}H_{50}O$. ^{1}H-NMR (400 MHz) and DEPT-Q NMR (100 MHz) in $CDCl_3$.

Compound (**3**): Yellowish white amorphous powder (50 mg), m.p. 289–291 °C, produced a positive reaction to $FeCl_3$ reagent. LC-HRMS $[M + H]^+$ *m/z*: 345.0602, R_t: 16.99 calculated for $C_{17}H_{12}O_8$. ^{1}H-NMR (400 MHz) and DEPT-Q NMR (100 MHz) in DMSO-d_6.

Compound (**4**): White amorphous powder (24 mg), m.p. 290 °C; the color of the spot was invisible in TLC and under UV but after spraying with *p*-anisaldehyde, it was violet. It gave a positive Libermann–Burchard's test indicating its steroidal or triterpenoidal nature and gave a positive with Molish's test indicating its glycosidic nature. LC-HRMS $[M + H]^-$ *m/z*: 575.3155, R_t: 25.82 calculated for $C_{35}H_{60}O_6$. ^{1}H-NMR (400 MHz) and DEPT-Q NMR (100 MHz) in DMSO-d_6.

3. Investigation of Ethyl Acetate Fraction of *E. abyssinica* J.F. Gmel

Chromatographic investigation of ethyl acetate fraction led to the isolation of seven compounds. The structure of the isolated compounds was elucidated using 1D, 2D NMR, and LC-HRMS. Compound (**5**): White crystalline

powder (17 mg), m.p. 198–200 °C, produced a positive reaction to $FeCl_3$ reagent. LC-HRMS $[M + H]^-$ *m*/*z*: 183.0301, R_t: 8.37 calculated for $C_8H_8O_5$. ^{1}H-NMR (400 MHz) and DEPT-Q NMR (100 MHz) in (CD_3OD).

Compound (**6**): White crystalline powder (14 mg), m.p. 258–263 °C, produced a positive reaction to $FeCl_3$ reagent. LC-HRMS $[M + H]^-$ *m*/*z*: 169.0143, R_t: 5.01 calculated for $C_7H_6O_5$. ^{1}H-NMR (400 MHz) in CD_3OD and DEPT-Q NMR (100 MHz) in (CD_3OD).

Compound (**7**): Yellow powder (10 mg), m.p. 172–174 °C, LC-HRMS $[M + H]^+$ *m*/*z*: 433.1125, R_t: 12.70 calculated for $C_{21}H_{20}O_{10}$. ^{1}H-NMR (400 MHz) and DEPT-Q NMR (100 MHz) in CD_3OD.

Compound (**8**): Yellow amorphous powder (12 mg), m.p. 179–183 °C, LC-HRMS $[M + H]^+$ *m*/*z*: 449.1074, R_t: 11.87 calculated for $C_{21}H_{20}O_{11}$. TLC investigation revealed an orange spot while it showed a deep purple spot under UV light, which became yellow–green when fumed with ammonia vapor but showed dark orange color with *p*-anisaldehde indicating its flavonoid-3-*O*-substituted nature. ^{1}H-NMR (400 MHz) and DEPT-Q NMR (100 MHz) in CD_3OD.

Compound (**9**): Yellowish white amorphous powder (25 mg), m.p. 297 °C, produced a positive reaction to $FeCl_3$ reagent. LC-HRMS $[M + H]^+$ *m*/*z*: 493.0970, R_t: 9.57 calculated for $C_{22}H_{20}O_{13}$. ^{1}H-NMR (400 MHz) and DEPT-Q NMR (100 MHz) in DMSO-d_6.

Compound (**10**): Off-white amorphous powder (16 mg), m.p. 180–182 °C, produced a positive reaction to $FeCl_3$ reagent. LC-HRMS $[M + H]^+$ *m*/*z*: 485.0921, R_t: 8.29 calculated for $C_{20}H_{20}O_{14}$. ^{1}H-NMR (400 MHz) and DEPT-Q NMR (100 MHz) in CD_3OD.

Compound (**11**): Yellowish white amorphous powder (45 mg), m.p. 267–268 °C, produced a positive reaction to $FeCl_3$ reagent. LC-HRMS $[M + H]^+$ *m*/*z*: 653.1704, R_t: 11.93 calculated for $C_{29}H_{32}O_{17}$. ^{1}H-NMR (400 MHz) and DEPT-Q NMR (100 MHz) in DMSO-d_6.

4. Investigation of *n*-Butanol Fraction of *E. abyssinica* J.F. Gmel

Chromatographic investigation of *n*-butanol fraction led to the isolation of one compound. The structure of the isolated compound was elucidated using ^{1}H-NMR, and LC-HRMS. Compound (**12**): Yellow amorphous powder (6 mg), m.p. 320–330 °C. UV λ_{max} (MeOH) nm: 225, 258, 347.5, ($AlCl_3$) 272.5, 297, 331, 421. LC-HRMS $[M + H]^+$ *m*/*z*: 449.1074, R_t: 11.87 calculated for ($C_{21}H_{20}O_{11}$). ^{1}H-NMR (400 MHz) and DEPT-Q NMR (100 MHz) in CD_3OD. All isolated compounds are represented in (**Figure 1**).

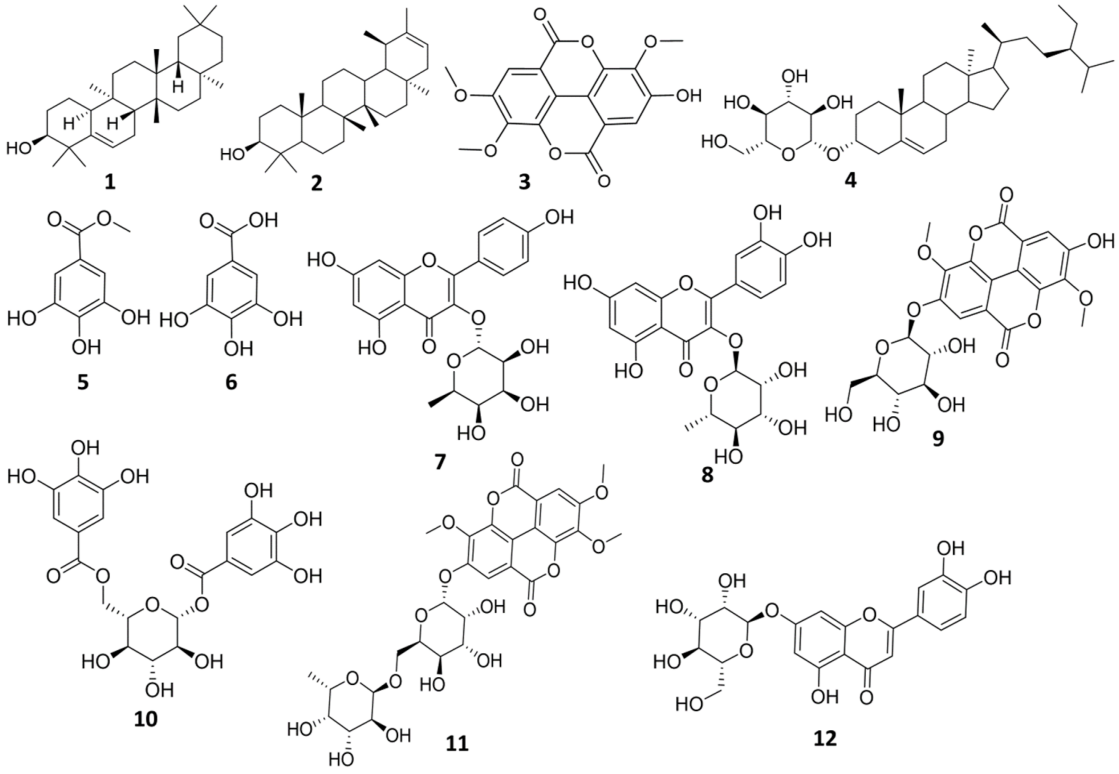

Figure 1. Structure of the isolated compounds from *E. abyssinica*.

5. Docking Study for Anti-Trypanosomal Activity

The results of docking procedures contained binding free energies Kcal/mol, binding affinity constant (*ki* in nm), distances (in Å) from the main residues, and type of interactions. Notably compounds **10**, **7**, **11**, **8,** and **12** in order, showed good binding affinity energies (from −18.9900 to −23.0767 Kcal/mol) when compared to the co-docked ligand suramin as a positive control (**Figure 2**). The main residues involved in the interaction between compounds and *T. brucei* PFK enzyme were Arg173, Ser341, Asn343, Lys226, Thr201, and Gly107 residues as well as Mg Atom (MG1002) that mark them as good candidates for *T. brucei* PFK inhibition, that could be used for the treatment of trypanosomiasis. Hydrogen acceptor and metal interactions were found to be the main formed interactions between compounds and the enzyme. 3D figures of the most active compounds via PyMOL 2.4 software were represented in (**Figure 3**).

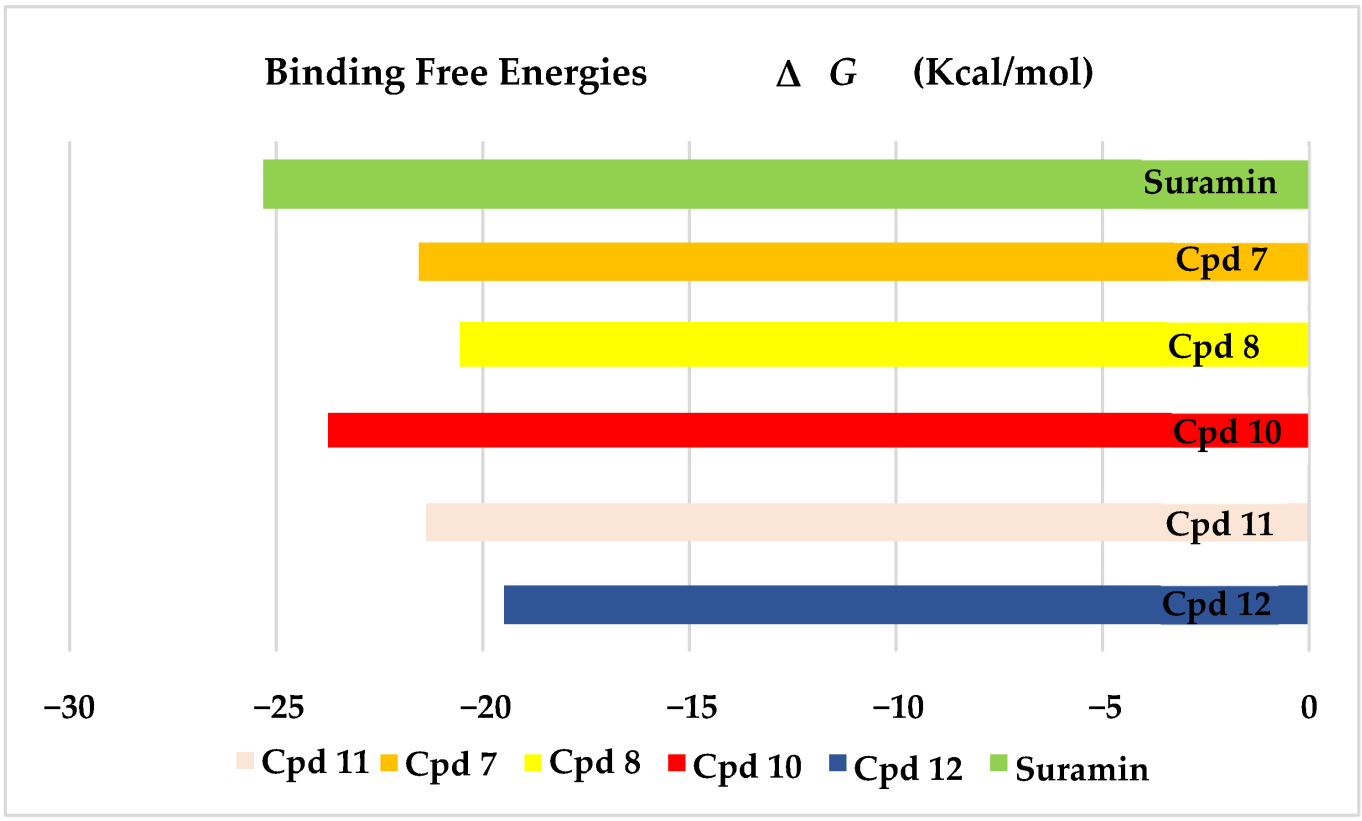

Figure 2. Binding free energy score of the most active isolated compounds and suramin with *T. brucei* PFK enzyme (PDB ID:3F5M).

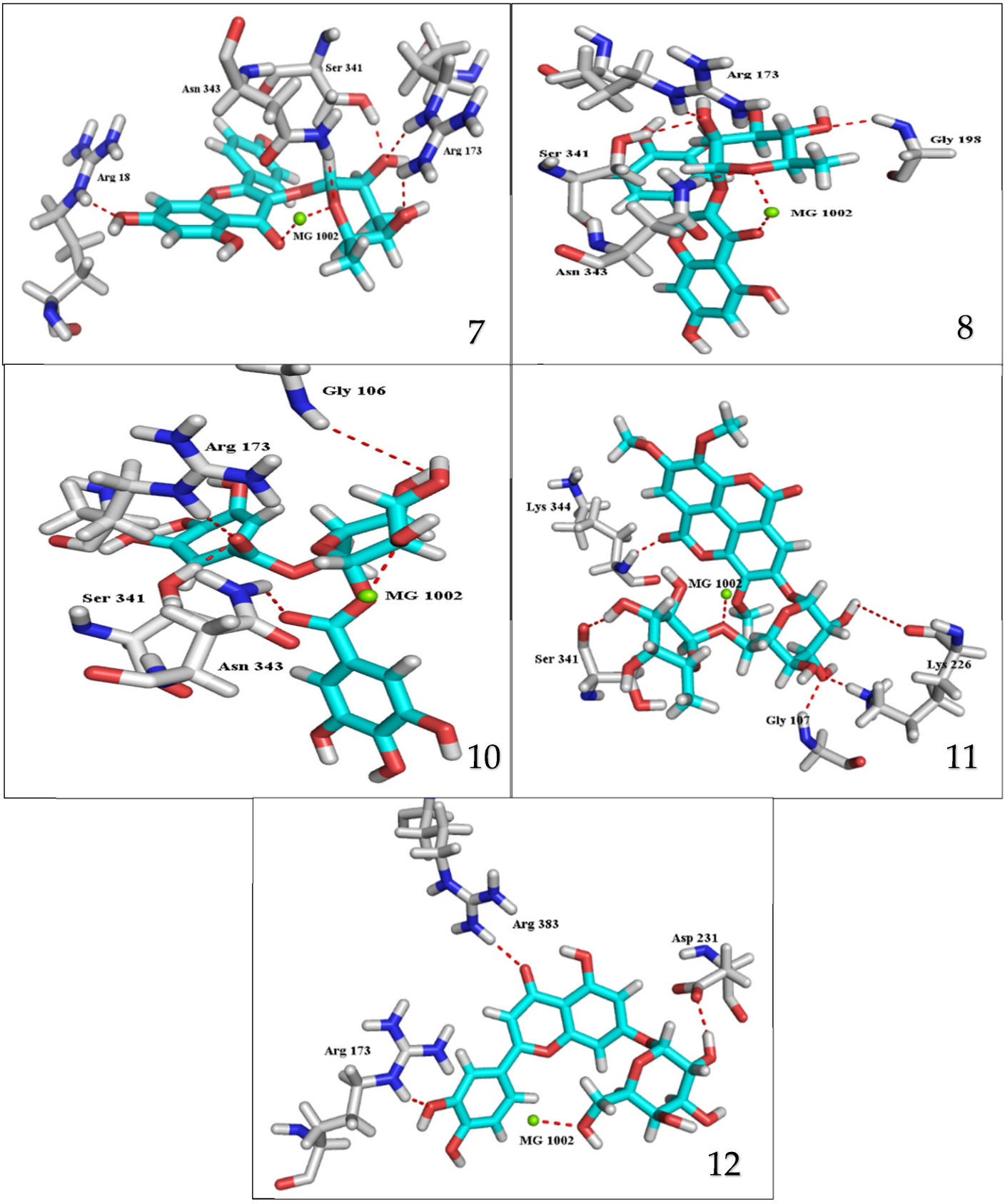

Figure 3. 3D interaction caption of the top docking pose of the most active isolated compounds.

6. Molecular Dynamics Simulations

With the aim of proofing the reliability of molecular docking results, further computational validation was achieved through a number of MDS experiments and binding free energy (ΔG) calculations on compound **10** (1,6-di-*O*-galloyl-d-glucose), as well as suramin. As seen in **Figure 4**, compound **10** was able to achieve stable binding inside the enzyme′s (i.e., phosphofructokinase, PDB ID:3F5M) active site with an average RMSD from the initial docking pose of 3.1 Å; however, it showed higher fluctuation in comparison with the standard drug suramin. Accordingly, it obtained a binding free energy value (ΔG) of −7.1 kcal/mol (ΔG of suramin was −8.8 kcal/mol).

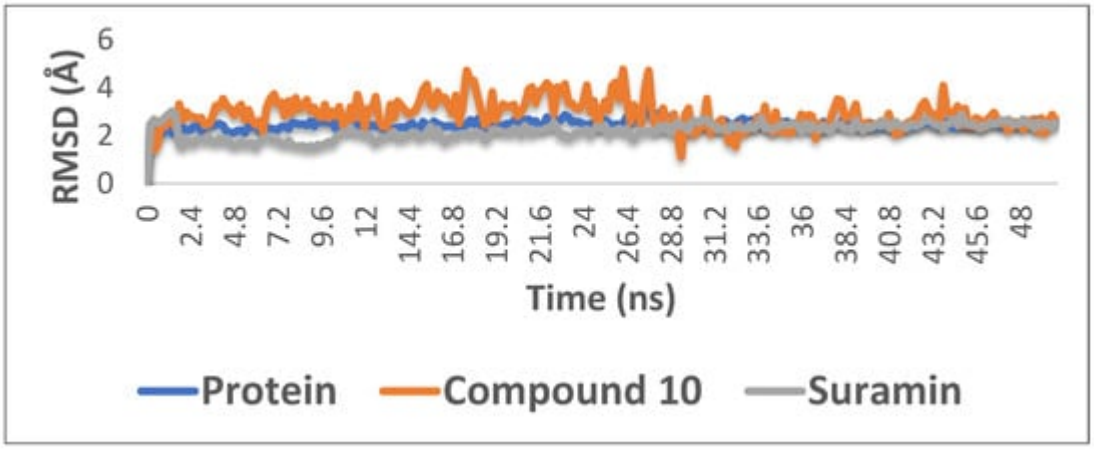

Figure 4. The RMSD curve from the molecular dynamics simulations of compound **10**. The X-axis represents the simulation time (in ps), while the y-axis represents the RMSD value (in nm).

7. Prediction of the Pharmacokinetic Properties and Toxicological Properties Using ADMET

After the molecular docking studies of 12 isolated compounds, the absorption, distribution, metabolism, elimination, and toxicity (ADMET) of the best dock scored compound along with suramin were evaluated (**Table 1**).

Table 1. ADMET properties of compound **10** and suramin.

	Properties	Compound 10	Suramin
Absorption	Caco-2 permeability (log Papp in 10^{-6} cm/s)	−1.682	−3.097
	HIA (% Absorbed)	15.64%	0
	P-glycoprotein substrate	Yes	Non
	P-glycoprotein I inhibitor	Non	Non
	P-glycoprotein II inhibitor	Non	Non
	Pure water solubility (log mol/L)	−2.895	−2.892
	Skin Permeability (log Kp)	−2.735	−2.735

	Properties	Compound 10	Suramin
Distribution	BBB Permeability (log BB)	−2.435	−4.438
	CNS permeability (log PS)	−4.668	−4.991
	VDss human (log L/kg)	1.614	−0.007
	Fraction unbound human (Fu)	0.347	0.379
Metabolism	CYP 2C19 inhibitor	Non	Non
	CYP 2C9 inhibitor	Non	Non
	CYP 2D6 inhibitor	Non	Non
	CYP 2D6 substrate	Non	Non
	CYP 3A4 inhibitor	Non	Non
	CYP 3A4 substrate	Non	Non
	CYP 1A2 inhibitor	Non	Non
Excretion	Total Clearance (log mL/min/kg)	0.47	−4.065
	Renal OCT2 substrate	Non	Non
Toxicity	Ames test	non-mutagen	non-mutagen
	Max. tolerated dose human (log mg/kg/day)	0.49	0.438
	Oral Rat Acute Toxicity LD_{50} (mol/kg)	2.515	2.482
	Oral Rat Chronic Toxicity LOAEL (log mg/kg-bw/day)	3.491	6.817
	hERG I inhibitor	Non	Non
	hERG II inhibitor	Yes	Yes
	T. pyriformis toxicity (log µg/L)	0.285	0.285
	minnow toxicity (log mM)	5.837	6.162

References

1. Ayyildiz, M.; Celiker, S.; Ozhelvaci, F.; Akten, E.D. Identification of Alternative Allosteric Sites in Glycolytic Enzymes for Potential Use as Species-Specific Drug Targets. Front. Mol. Biosci. 2020, 7, 88.
2. Luisi, G.; Carradori, S. New Compounds for the Management of Trypanosoma brucei Infection. In Topics in Medicinal Chemistry; Springer: Berlin/Heidelberg, Germany, 2021.
3. EL-Fiky, F.; Asres, K.; Gibbons, S.; Hammoda, H.; Badr, J.; Umer, S. Phytochemical and Antimicrobial Investigation of Latex from Euphorbia abyssinica Gmel. Nat. Prod. Commun. 2008,

3, 1505–1508.

4. El-Hawary, S.S.; Mohammed, R.; Tawfike, A.F.; Lithy, N.M.; AbouZid, S.F.; Amin, M.N.; Abdelmohsen, U.R.; Amin, E. Cytotoxic activity and metabolic profiling of fifteen Euphorbia Species. Metabolites 2021, 11, 15.
5. Muluye, A.B.; Desta, A.G.; Abate, S.K.; Dano, G.T. Anti-malarial activity of the root extract of Euphorbia abyssinica (Euphorbiaceae) against Plasmodium berghei infection in mice. Malar. J. 2019, 18, 261.
6. Jabalia, N.; Kumar, A.; Kumar, V.; Rani, R. In Silico Approach in Drug Design and Drug Discovery: An Update. In Innovations and Implementations of Computer Aided Drug Discovery Strategies in Rational Drug Design; Springer: Singapore, 2021; pp. 245–271.
7. Kanapeckaitė, A.; Beaurivage, C.; Jančorienė, L.; Mažeikienė, A. In silico drug discovery for a complex immunotherapeutic target-human c-Rel protein. Biophys. Chem. 2021, 276, 106593.
8. El-Hawary, S.S.; Lithy, N.M.; Amin, E.; AbouZid, S.F.; Mohammed, R. Anti-trypanosomal activity and DNA fingerprinting of fifteen Euphorbia species using ISSR and SCoT markers. Beni-Suef Univ. J. Basic Appl. Sci. 2021, 10, 54.